Article

Glassy PEEK-WC vs rubbery Pebax®1657 polymers: effect on the gas transport in CuNi-MOF based mixed matrix membranes

Elisa Esposito[1*], Rosaria Bruno[2], Marcello Monteleone[1], Alessio Fuoco[1], Jesús Ferrando-Soria[3], Emilio Pardo[3], Donatella Armentano[2], Johannes Carolus Jansen[1*]

[1]Institute on Membrane Technology, CNR-ITM, Via P. Bucci 17/C, 87036 Rende (CS), Italy. e.esposito@itm.cnr.it (E.E.); m.monteleone@itm.cnr.it (M.M.); a.fuoco@itm.cnr.it (A.F.)
[2] Dipartimento di Chimica e Tecnologie Chimiche (CTC), Università della Calabria, Rende 87036, Cosenza, Italy. rosaria.bruno@unical.it (R.B), donatella.armentano@unical.it (D.A.).
[3] Departamento de Química Inorgánica, Instituto de Ciencia Molecular (ICMol), Catedrático José Beltrán Martínez, 2, Universidad de Valencia, 46980 Paterna, Valencia, Spain. jesus.ferrando@uv.es (J.F.); emilio.pardo@uv.es (E.P.)

* Correspondence: e.esposito@itm.cnr.it (E.E.), johannescarolus.jansen@cnr.it (J.C.J.); +39-0984-492008 (E.E.) +39-0984-492031(J.C.J.)

Received: date; Accepted: date; Published: date

Abstract: Mixed matrix membranes (MMMs) are seen as promising candidates to overcome the fundamental limit of polymeric membranes, known as the so-called Robeson upper bound, which defines the best compromise between permeability and selectivity of neat polymeric membranes. To overcome this limit, the permeability of the filler particles in the MMM must be carefully matched with that of the polymer matrix. The present work shows that it is not sufficient to match only the permeability of the polymer and the dispersed phase, but that one should consider also the individual contributions of the diffusivity and the solubility of the gas in both components. Here we compare the gas transport performance of two different MMMs, containing the metal organic framework CuNi-MOF in the rubbery Pebax®1657 and in the glassy poly(ether-ether-ketone) with cardo moiety, PEEK-WC. The chemical and structural properties of MMMs were investigated by means of FT-IR spectroscopy, scanning electron microscopy and EDX analysis. The influence of MOF on the mechanical and thermal properties of both polymers was investigated by tensile tests and differential scanning calorimetry, respectively. The MOF loading in Pebax®1657 increased the ideal H_2/N_2 selectivity from 6 to 8 thanks to an increased H_2 permeability. In general, the MOF had little effect on the Pebax®165 membranes because an increase in gas solubility was neutralized by an equivalent decrease in effective diffusivity. Instead, the addition of MOF to PEEK-WC increases the ideal CO_2/CH_4 selectivity from 30 to ~48 thanks to an increased CO_2 permeability (from 6 to 48 Barrer). The increase in CO_2 permeability and CO_2/CH_4 selectivity is maintained under mixed gas conditions.

Keywords: Mixed matrix membrane, glassy polymer, rubbery polymer, PEEK-WC, Pebax®1657, Gas separation, CuNi-MOF

1. Introduction

The research field on materials for gas separation membranes is constantly expanding due to the pressing industrial request for more performing materials to employ in gas treatment, such as hydrogen recovery (H_2/CO_2) [1], oxygen-enriched air production (O_2/N_2) [2,3], biogas up-grading [4,5] and natural gas treatment (CO_2/CH_4) [6], and post combustion carbon capture from flue gas (CO_2/N_2) [7]. This increasing interest is dictated by the advantages of membrane technology compared to traditional gas separation techniques. Gas separation by means of membrane technology is an economic process, it is easily scalable and it can be used in non-drastic temperature and pressure conditions, which are more environmentally friendly. Despite numerous efforts to develop new materials for gas separation, the membrane market still need to overcome some challenges. In fact, higher permeable rubbery polymers present low selectivity and the high selective glassy polymers are less permeable. To overcome this trade-off, extensively reported by Robeson in 1991 and in 2008 [8,9], research is focusing on the design and development of hybrid membranes based on the combination of two different materials, in order to get advantages of both [10]. According to this concept, a valid strategy is the embedding porous metal-organic frameworks (MOFs) in the polymer matrix in order to obtain mixed matrix membranes (MMMs) with enhanced gas transport properties [11–13]. MOFs are an attractive new class of microporous materials built by the combination of metal atoms/clusters with a wide variety of organic ligands, which can be specifically designed for improving the compatibility with the organic polymer phase and with high specify for gases [14,15]. The gas transport in polymer membranes occurs following the solution-diffusion mechanism in which permeability and selectivity are determined by kinetic parameters (diffusion) and thermodynamic factors (solubility), via $P = D * S$; $\alpha_{x/y} = D_x/D_y * S_x/S_y$. The addition of MOFs can improve the gas transport properties of the neat polymer by influencing these two parameters [10]. The diffusion, being a kinetic phenomenon, is strongly linked to the free volume of polymer materials and to the molecular size of the penetrating species. In the MOFs, the link between metals and organic units forms a three-dimensional structure with cages having well-defined shape and size, which can improve free volume elements of matrix, increasing gas transport in terms of permeability. At the same time, the cages of MOF forming a preferential pathway for a specific gas can act as a molecular sieve increasing membrane selectivity. On the contrary, the main factor that determines the solubility in a polymer matrix is the ability of the penetrant gases to condense, which in turn is correlated with the interactions that occur between the gas and the matrix of membrane. MOFs chemical structure can be easily designed or functionalized synthetically in order to improve its affinity for specific gases [16]. In this case, the membrane permeability is expected to improve as a consequence of an increased contribution in solubility due to the gas condensability in the MOF. Furthermore, the introduction of chemical groups with a specific affinity to one gas in a mixture will also increase its selectivity. The choice of the materials combination for MMMs preparation must be made on the basis of specific physical and chemical properties, in order to tailor in advance, the membrane for a desired gas separation. For this reason, it is necessary to understand how the addition of MOF can influence the gas transport properties of different polymers, rubbery or glassy.

In this work, the gas transport properties for MMMs prepared by embedding the same oxamate-based MOF in two different polymers, Pebax®1657 rubbery polymer and PEEK-WC glassy polymer, will therefore be investigated. The oxamate-based MOF, previously reported [17], with formula $Ni^{II}_2\{Ni^{II}_4[Cu^{II}_2(Me_3mpba)_2]_3\}\cdot 54H_2O$ (where Me_3mpba is the N,N′-2,4,6-trimethyl-1,3-phenylenebis (oxamate) ligand), has already shown interesting gas separation properties [18].

Single-crystal X-ray diffraction measurements unveil the crystal structure of CuNi-MOF. The anionic $Ni^{II}_6Cu^{II}_6$ open-framework structure, exhibits a pillared square/octagonal layer architecture, where nickel(II) and copper(II) ions are located on the vertices and midpoints of the edges, respectively, featuring three types of pores, different in size and shape, propagating along the c axis and enfolding up to 60% of the total lattice volume. Free nickel(II) cations are further accommodated within pores of the MOF. It consists of regularly spaced, small almost square sized pores (virtual diameter of ca 0.4 nm) and two kinds of hydrophobic and hydrophilic octagonal pores (Figure 1)

resulting from the different disposition of the trimethyl-substituted phenylene spacers, pointing inwards or outwards of the voids, which accounts for their virtual diameters of ca. 1.5 and 2.2 nm, respectively (Figure 1).

PEEK-WC is a glassy poly(ether-ether-ketone) with a cardo group in the polymer backbone, which makes it soluble in various common organic solvents. It has been used extensively in membrane preparation and characterization under the names PEEK-WC, PEEKWC or PEK-C [19]. Membranes have been prepared in the form of hollow fibres for liquid filtration [20] and as flat films for liquid filtrations [21] or for gas separation [22–24] and numerous other applications [19]. In this work, we take advantage of its good solubility in chloroform for the preparation of mixed matrix membranes by the solvent evaporation method. PEEK-WC presents a high selectivity but a too low permeability to be interesting as a material for industrial application. For this reason, different researchers have tried to improve its permeability without loss in selectivity by means of nanoparticle addition. An extensive protocol to obtain MMMs based on PEEK-WC, embedding NaA (LTA) zeolite, was developed in order to improve gas separation parameters [25]. However, no one procedure have enhanced gas transport properties of neat polymer and a decrease in selectivity was observed probably due to a presence of defects at interface between polymer and zeolite. Some methods have been developed in order to further improve the adhesion of PEEK-WC for 3D-mesoporous nanoparticles. For example, the MIL-101 was functionalized with sulfonic acid group for further increase the affinity for polymer matrix. The resulted membranes have shown an improved CO_2 permeability and CO_2/gas selectivity. The increased selectivity was mainly attributed to the increased polar interaction between CO_2 and sulfonic acid groups as well as the good filler–polymer interface compatibility [26].

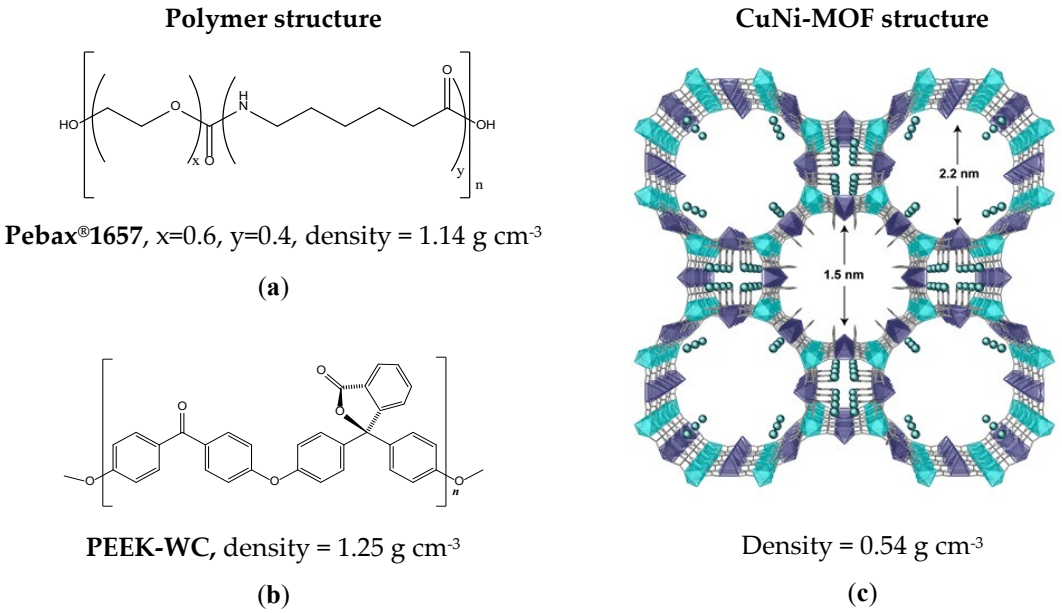

Pebax®1657, x=0.6, y=0.4, density = 1.14 g cm^{-3}

(**a**)

PEEK-WC, density = 1.25 g cm^{-3}

(**b**)

Density = 0.54 g cm^{-3}

(**c**)

Figure 1. Chemical structure and density of (**a**) Pebax®1657, (**b**) PEEK-WC; and (**c**) CuNi-MOF. Cu and Ni atoms from the network are represented by cyan and green polyhedra, respectively, whereas organic ligands are depicted as sticks. Green spheres represent Ni^{2+} metal ions in pores.

Pebax®1657 is a thermoplastic elastomer multiblock-copolymer containing linear chains of rigid polyamide segments interspaced with flexible polyether segments. The hard polyamide (PA) blocks supply mechanical strength and the presence of the polar ethylene oxide (PEO) group, increases the affinity for CO_2, allowing a good CO_2/non-polar (H_2, N_2, and CH_4) species separation and

permselectivity. Several membranes have been prepared in the form of composite hollow fibre membranes [27–29], hybrid and mixed matrix membranes for gas separation [30,31,40,32–39]. Mixed matrix membranes based on amine-functionalized and pristine MIL-53(Al) in Pebax® MH-1657 have shown an increased CO_2 separation and the higher permeability and selectivity (PCO_2 100 Barrer and $\alpha CO_2/CH_4$=17; CO_2/N_2=50), was attributed to high porosity introduced by the presence of the MOF, as well as the selective adsorption of CO_2 inside the MOF [37]. Composite hollow fiber membranes with a selective layer of Pebax®1657 and different functionalized Uio-66 MOF have demonstrated a simultaneous improvement in gas permeance and selectivity. The enhanced selectivity was attributed to an increased rigidity of polymer matrix due to formation of hydrogen bond between MOF and Pebax®1657 polymer chains [41]. Pebax®1657 containing Cu_3BTC_2-MOF have shown an increased CO_2/CH_4 ideal selectivity about 15% compared to the neat Pebax®1657 [42]. The improvement in selectivity was attributed to the improvement in the CO_2 solubility, which having a strong quadrupole moment presents higher affinity with unsaturated Cu sites than CH_4, leading to a higher CO_2 permeability. In this work, the CuNi-MOF was dispersed in the Pebax®1657 rubbery polymer and in the PEEK-WC glassy polymer, which presenting Cu site and well-defined cages (1.5 nm and 2.2 nm), is expected to influence at the same time solubility and diffusion coefficient. The aim is to understand the main factors that determine the behavior when a MOF is dispersed within a glassy or rubbery polymeric matrix. FT-IR, EDX, DSC and SEM analysis, investigate the potential chemical interaction between CuNi-MOF and polymers. Besides pure gas permeability tests with six different gases were carried out to obtain a general understanding of the MMM performance, while permeation tests were also carried out with binary CO_2/N_2 and CH_4/CO_2 gas mixtures to evaluate its potential performance in a real separation process. These two gas pairs simulate flue gas in view of potential use of the membranes in CO_2 capture, and biogas in view of the potential exploitation of renewable energy in a strongly emerging market.

2. Materials and Methods

Pebax®1657, a poly(ethylene-oxide) (PEO) and poly[imino(1-oxohexamethylene)] (PA6) multi-block co-polymer in the molar ratio 60/40, was kindly provided by Arkema in the form of pellets.

PEEK-WC was provided as a powder by the Institute of Applied Chemistry, Changchun, China, and was used as received, without further purification.

The CuNi-MOF was obtained as crystalline phase through a double cation-exchange reaction in the solid state by immersing crystals of $Mg^{II}_2\{Mg^{II}_4[Cu^{II}_2\text{-}(Me_3mpba)_2]_3\}\cdot 45H_2O$ in saturated aqueous solutions of $Ni(NO_3)_2\cdot 6H_2O$ for several weeks [43]. Alternatively, a large scale synthesis of $Ni^{II}_2\{Ni^{II}_4[Cu^{II}_2(Me_3mpba)_2]_3\}\cdot 54H_2O$ (2) was carried out by direct reaction of two aqueous solutions of $Na_4[Cu_2(Me_3mpba)_2]\cdot 4H_2O$ (0.1 mol) and $Ni(NO_3)_2\cdot 6H_2O$ (0.13 mol) in water and subsequent addition, after filtration and re–suspension in water of the resulting compound, of 0.067 mol of $Ni(NO_3)_2\cdot 6H_2O$ (Yield 99 %) [17].

2.1. Membranes preparation

Mixed matrix membranes were prepared loading different concentrations of CuNi-MOF (9 wt%, 17 wt%, 23 wt%) in Pebax®1657 and in PEEK-WC. The Pebax®1657 solution at 10 wt% was prepared by swelling polymer pellets in a mixture of distilled water and ethanol (ratio 30:70 wt/wt) at room temperature overnight. Then a homogeneous dope solution was obtained by heating to 80 °C under magnetic stirring for at least 10 min. The CuNi-MOFs were dispersed and sonicated in water-ethanol mixture for 30 min and subsequently added to the Pebax®1657 solution under magnetic stirring. While, homogenous solution at 5 wt% of PEEK-WC was obtained by dissolving the polymer powder in chloroform at room temperature for 24 h. Concurrent the CuNi-MOFs were separately dispersed in chloroform and sonicated in an ultrasonic bath for 30 min before filtering the PEEK-WC solution through glass wool into the suspension. One hour of mechanical stirring and 30 minutes of sonication make homogeneous each solution. The resulting solutions were cast into levelled flat Teflon petri-dish and left to evaporate over 2-3 days. The MMMs produced were dried in oven at 70°C under vacuum condition for 24 h.

2.2. *Membranes characterization*

2.2.1 Structural characterization

Chemical and morphological analysis of membranes were performed by scanning electron microscopy (SEM) (Phenom Pro X desktop SEM, Phenom-World. The samples for cross-section SEM characterization were prepared by freeze-fracturing in liquid nitrogen. Samples were analyzed without sputter coating with gold. Elemental analysis was performed with the Phenom- Pro X desktop SEM and which is equipped with an energy dispersive X-ray spectroscopy detector (EDX).

Infrared spectroscopy (FT-IR) analyses were performed by means of Spectrum Spotlight Chemical Imaging Instrument (PerkinElmer) in ATR mode.

2.2.2. Thermal and mechanical characterization

DSC analysis was carried out using a Pyris Diamond Differential Scanning Calorimeter (Perkin Elmer, USA) equipped with an intracooler refrigeration system. Samples of 15-20 mg. Unless specified otherwise, three cycles were performed. The PEEK-WC samples were first heated from -60 °C to 300 °C, kept at this temperature for 1 min, and cooled down to 0 °C where they were kept for 5 min. In the second run, the samples were heated up again to 300 °C. The DSC runs were performed at a scan rate of 15 °C min^{-1}. Before the measurements, the samples were kept at 50°C under vacuum for one night in order to remove possibly adsorbed water. The Pebax®1657-based samples were tested by an identical method in the range from -40°C → 220°C → -75 °C → 225°C.

Tensile tests were carried out at room temperature on a single column Universal Testing Machine, Zwick/Roell model Z2.5, equipped with a 50 N load cell and pneumatic clamps. Surface of one flat clamp was covered with adhesive rubber to avoid slipping or damage of the samples, while second clamp had convex surface to increase the local pressure and to avoid the extraction of the sample. The average value and the standard deviation of the Young's modulus, the tensile strength and the maximum deformation were determined on a series of at least four samples. The sample width was 5 mm, the grip-to-grip distance 40 and 30 mm for Pebax®16 and PEEK-WC, respectively. The test were carried out at a deformation rate 20 mm min^{-1} (200 % min^{-1}) for Pebax®1657-based samples and 6 mm min^{-1} (20 % min^{-1}) for PEEK-WC-based samples.

2.2.3 Single gas permeation method

Single gas permeation tests were carried out at 25 °C and at a feed pressure of 1 bar, using a fixed-volume pressure increase instrument (ESSR), described elsewhere [44]. Permeability coefficients, *P*, and diffusion coefficients, *D*, were determined by the time-lag method [45]. The permeability coefficient, P, is calculated from the permeation curve in steady state described by:

$$P_t = P_0 + (dp/dt)_0 \cdot t + \frac{RT \cdot A}{V_p \cdot V_m} \cdot \frac{p_f \cdot p}{\ell} \left(t - \frac{\ell^2}{6D}\right) \quad (1)$$

the last term in (Eq. 1) represents the so-called permeation time lag, Θ, which is inversely proportional to the diffusion coefficient of the gas:

$$\Theta = \frac{\ell^2}{6D} \quad (2)$$

the approximate gas solubility coefficient, S, was obtained indirectly as the ratio of the permeability to the diffusion coefficient by assuming the solution-diffusion transport mechanism:

$$S = P/D \quad (3)$$

Permeabilities are reported in Barrer [1 Barrer=10^{-10} cm^3 (STP) cm cm^{-2} s^{-1} cm Hg^{-1}].

2.2.3 Mixed gas permeation measurement

Mixed gas permeation tests were carried out using a custom made constant pressure/variable volume instrument, described in detail elsewhere [46], equipped with a quadrupole mass filter (HPR-

20 QIC Benchtop residual gas analysis system, Hiden Analytical). Measurements were performed from 1 to 6 bar(a) with two binary gas mixtures of CO_2/N_2 (15:85 vol%) and CO_2/CH_4 (35:65 vol%), simulating flue gas and biogas, respectively. Argon was used as a sweeping gas and as the internal standard for the calculation of the permeate gas composition.

3. Results and discussion

3.1. Chemical and morphological characterization

The MOF loading in polymer matrix, was evident by distinctive colour of obtained membranes, and it was accurately confirmed by the EDX analysis, which reveals the attendance of Cu and Ni metals in both Pebax®1657 and PEEK-WC polymers (See SI, Figure S1-a and b, respectively). The chemical characterization of neat membranes and MMMs, as well the interaction between polymer chains and nanoparticles were investigated by FTIR-ATR. Figure 2b and Figure 2d shows the spectrum for neat Pebax®1657 and for Pebax®1657/CuNi-MOF membranes. The functional groups of Pebax®1657 give characteristic peaks at 3297 cm^{-1} for N-H group, at 2943 and 2859 cm^{-1} attributed to the asymmetric and symmetric stretching of the C-H bound, 1731 cm^{-1} for the symmetric stretches of carboxylate R-O-C=O, while asymmetric R-O-C=O at ca. 1430, 1636 cm^{-1} for H-N–C=O and 1099 cm^{-1} for –C–O–C.

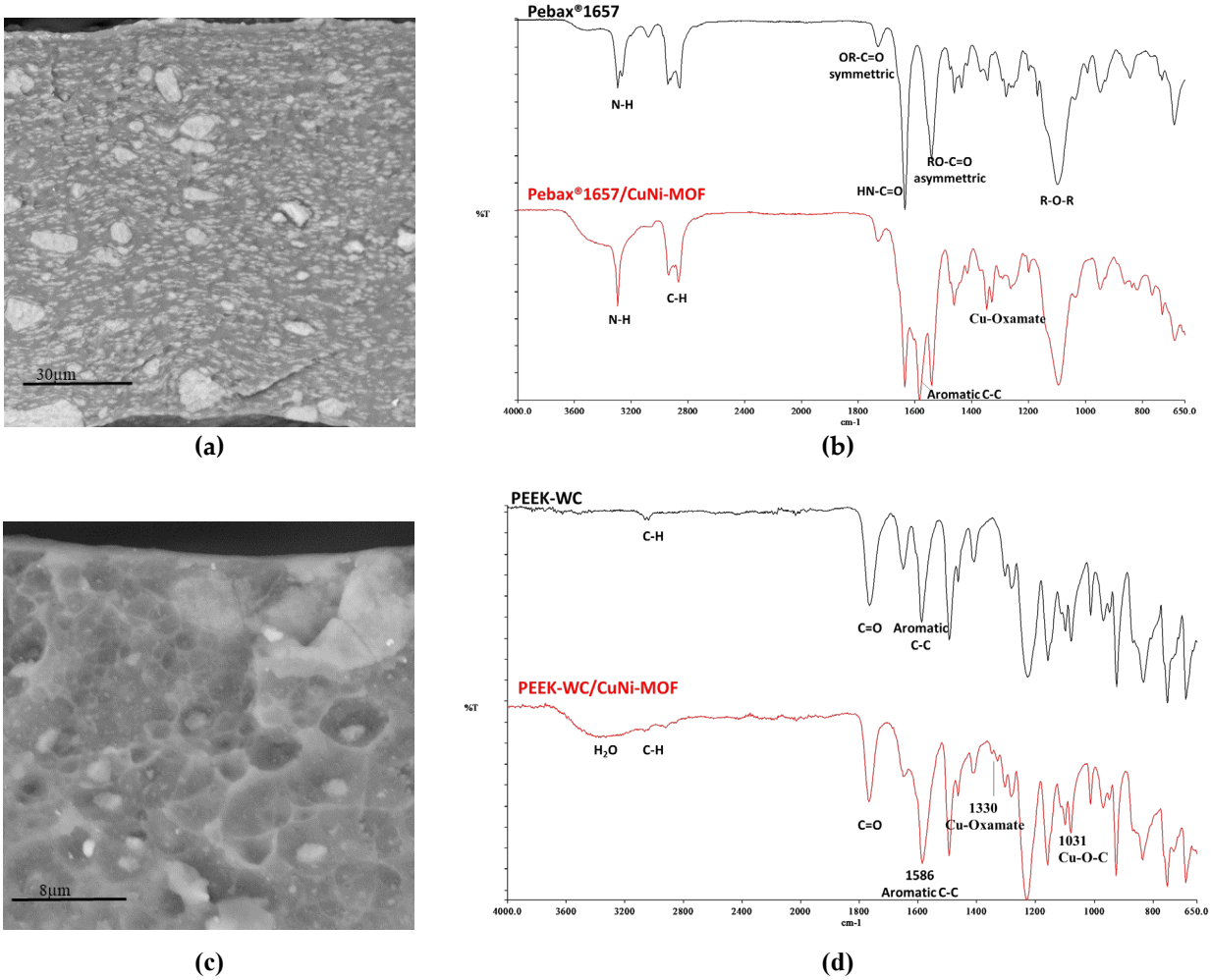

Figure 2. SEM image of the samples showing the interface between MOF and polymer phase (**a**) for Pebax®1657 and (**c**) PEEK-WC. FT-IR of neat polymer and MMMs with 23 wt% of CuNi, for Pebax®1657 (**b**) and PEEK-WC (**d**).

In the spectrum of Pebax®1657/CuNi-MOF characteristic peaks appear at 1578 cm^{-1} due to C–C aromatic band of MOF's phenylene, at 1608 cm^{-1} for stretching of oxamate ligand of MOF and a peak at 1330 cm^{-1}, which could be considered diagnostic of the presence of bridging oxamate between Cu and Ni [47]. Finally, the characteristic peaks between 2900 cm^{-1} and 2800 cm^{-1} due to the symmetric and asymmetric C-H stretching are slight shifted to lower wavelengths confirming the interaction of hydrogen bonds at the interface between MOF and Pebax®1657, as it was also see by Khosravi et al. for Pebax1657/CuBTC mixed matrix membranes [48]. Figure 2d offers a comparison of PEEK-WC membrane and PEEK-WC/CuNi spectrum. The functional groups of PEEK-WC give characteristic peaks at 3052 cm^{-1} and 3075 cm^{-1} for aromatic C–H stretch, at 1767 cm^{-1} for ketonic and esteric C=O stretching, and at 1589 cm^{-1} for C–C aromatic band [49]. In PEEK-WC/CuNi the peak for C-C aromatic band is shift on the lower wavelengths probably due to the π···π stacking interaction between benzene rings of polymers and MOF. In fact, when the ring is very conjugated, a weak band can be observed at around 1580 cm^{-1}, such as it is visible from the PEEK-WC/CuNi spectrum. While, the peaks due to the stretch of aromatic C–H appear to be totally fused with the water peak (3370 cm^{-1}) that reveals the relatively hydroscopic nature of the MOFs. The interaction between the Pebax®1657 and CuNi-MOF was also confirmed by SEM analysis, and in the enlarged particular of Figure 2a it is possible to see that polymer phase of Pebax®1657creates a sort of circular compressed polymer region around the MOF, which Koros defined as "Case I matrix rigidification". On the other hand, the distribution of MOF in the PEEK-WC polymer produces a defined and regular network structure (Figure 2c) with a homogenous dispersion of nanoparticles without significant sedimentation across the membranes (See SI Fig. S-2). Instead, the addition of MOFs in Pebax®1657 shows no significant agglomeration at lowest 9 wt% that becomes more significant at highest 29 wt% concentration.

3.2 Mechanical and thermal properties

All membranes are dense mixed matrix membranes with good mechanical resistance for handling. The results of the tensile tests, performed on the nanocomposite films obtained on the series with different concentration of CuNi-MOFs in Pebax®1657 and in PEEK-WC are shown in Figure 3. The PEEK-WC presents a Young's module about 1.14 GPa [50] and Pebax®1657 has a Young's module about 0.10 GPa [51]. In both polymers, the loading of CuNi-MOF increases the Young's modulus. The increase of Young's modulus indicates an increase of stiffness for both polymers increasing the MOF concentrations. The glassy PEEK-WC presents a higher modulus compared to the rubbery Pebax®1657 as expected and it remains higher even when MOF concentration was increased. On the other hand, the maximum deformation is higher in the more flexible MMMs based on the rubbery Pebax®1657 compared to the MMMs based on the rigid glassy PEEK-WC.

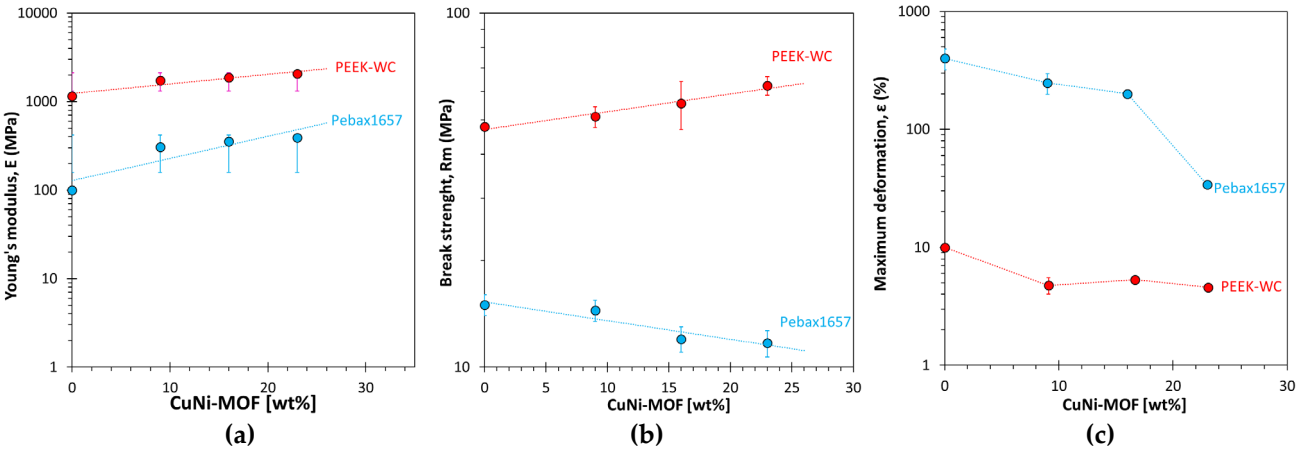

Figure 3. Young's modulus (a), tensile strength (b) and maximum deformation (c) as a function of the CuNi-MOF concentration in Pebax®1657 and PEEK-WC. Values of the neat PEEK-WC [50] and Pebax [51] samples from the literature. Trend lines are given as a guide to the eye.

The break strength decreases for Pebax®1657/CuNi membranes indicating that the membranes become weaker compared to the neat polymer. On the contrary, the break strength increases for PEEK-WC/CuNi membranes, suggesting a good adhesion between MOF and polymer that makes the MMMs stronger than neat PEEK-WC membrane. The thermal properties of the membranes were studied by DSC analysis and the results are displayed in Figure 4. For neat Pebax®1657 the two dominant endothermal peaks at 19 °C and 200 °C are attributed to the fusion of the crystalline fraction of the soft poly(ethylene oxide) (PEO) blocks and the hard polyamide (PA) blocks, respectively. In the presence of MOF, the melting enthalpy of both PEO and PA decrease. However, the peak maximum shifts to higher temperature, indicating that the MOF stabilizes the crystalline PEO and that it mainly interacts with this phase. On the other hand, no significant changes occur in the glass transition temperature of PEEK-WC at 230 °C as function of the MOF concentration.

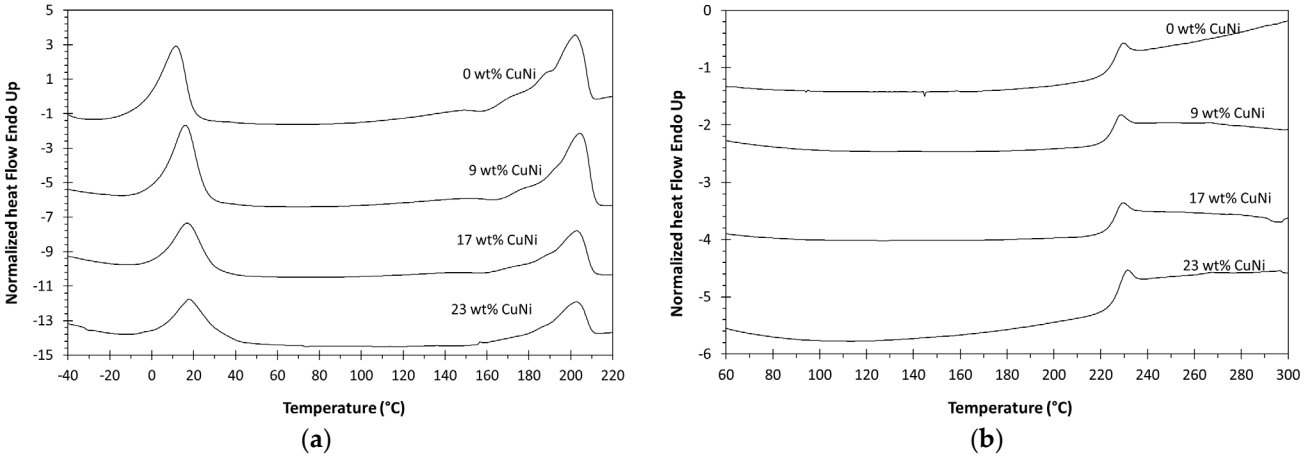

Figure 4. DSC thermograms for membrane of (**a**) neat Pebax1657 and (**b**) neat PEEK-WC and MMMs with different concentration of CuNi-MOF during the second eating.

3.3 Pure gas transport properties

Single gas permeation experiments were carried out in the order H_2, O_2, N_2, CH_4 and CO_2 at 25°C but repeated experiments with N_2 and O_2 at the end of the cycle were identical and revealed no structural changes in the material. An overview of the results of the Pebax®1657-based MMMs and PEEK-WC based MMMs with different filler loadings is given in Figure 5 and Figure 6, respectively. All permeability, diffusivity and solubility data, and their respective selectivities, are given in the supporting information (See SI Table 2 and 3). The dispersion of CuNi-MOF does not produce a substantial change in permeability of the rubbery Pebax®1657. The most permeable species is CO_2, confirming a solubility controlled transport ($CO_2 > H_2 > CH_4 > O_2 > N_2$), typical for the rubbers (Figure 5a). A remarkably strong decrease in the effective diffusion coefficients of all gases as function of the MOF loading (Figure 5b), is balanced by a proportional increase in their solubility coefficients (Figure 5c). This results in a similar permeability and selectivity (Figure 5d) for MMMs as in the neat Pebax®1657, with the only exception of the H_2/CH_4 gas pair, which suggests a favourable effect of the MOF on the size-selectivity. This is confirmed by the slight increase in the diffusion selectivities (Figure 5e), apparently because the MOF's provide preferential diffusion paths for smaller gases.

While the gas solubility upon addition of the MOF to Pebax increases as expected, given the generally high sorption capacity of MOFs for gases, it was not expected that this increase was more or less similar for all gases, and it was even less expected the porous fillers would effectively lead to a decrease in the diffusion coefficient. The explanation is that the filler does not effectively decrease the diffusion coefficient in the membrane, but the highly sorbing MOF transforms the permeation experiment in a sort of breakthrough experiment. The reason for the apparently slower diffusion is the accumulation of the gas inside the pores of the filler, similar to the phenomenon of immobilizing adsorption [52,53], but in this case it has virtually negligible net effect on the permeability.

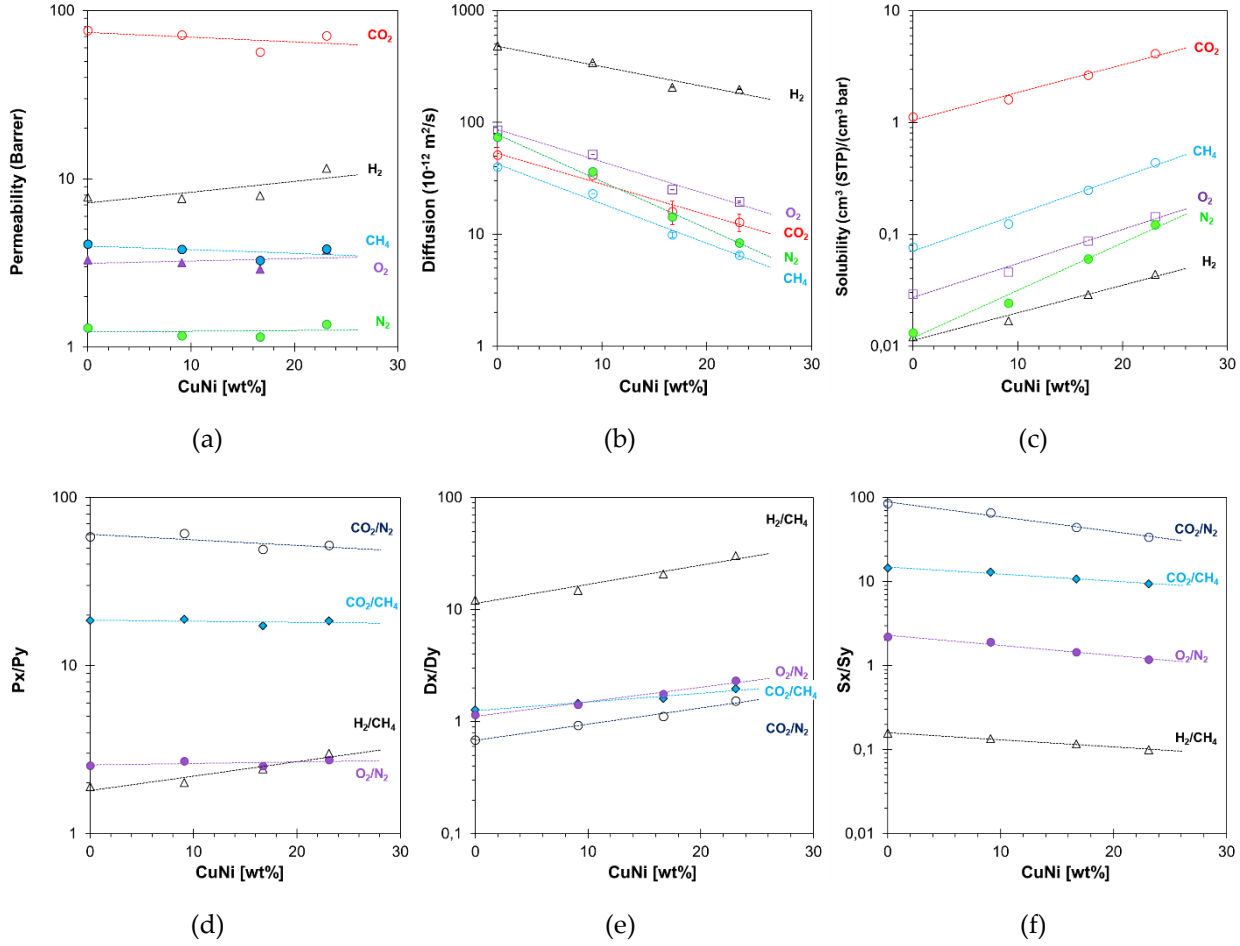

Figure 5. (**a**) Permeability, (**b**) diffusivity and (**c**) solubility coefficients, and their respective selectivity towards N_2 (**d, e, f**) for each gas as functions of the weight percentage of CuNi-MOF in Pebax®1657.

In contrast to the effect in Pebax®1657, CuNi-MOF causes a drastic increase in the gas permeability for all gases as function of MOFs loading in the glassy PEEK-WC, and the order of permeation obeys that of the diffusion controlled gas transport mechanism with $H_2 > CO_2 > O_2 > N_2 > CH_4$, typical for glassy polymers (Figure 6a). The increase in permeability is a direct consequence of an increase in diffusion coefficient (Figure 6b), whereas there is no substantial change in solubility coefficient (Figure 6c). The enhanced diffusion clearly indicates transport within the pore structure of CuNi-MOFs, which increases the total free volume of MMMs promoting the gas diffusion for all gases. The presence of MOF with chemical groups having a high affinity for CO_2, increase its solubility, its CO_2/CH_4 and CO_2/N_2 solubility selectivity (Figure 6f), and ideal selectivity for these two gas pairs (Figure 6d). Instead, the diffusion selectivity is not strongly affected by CuNi-MOF.

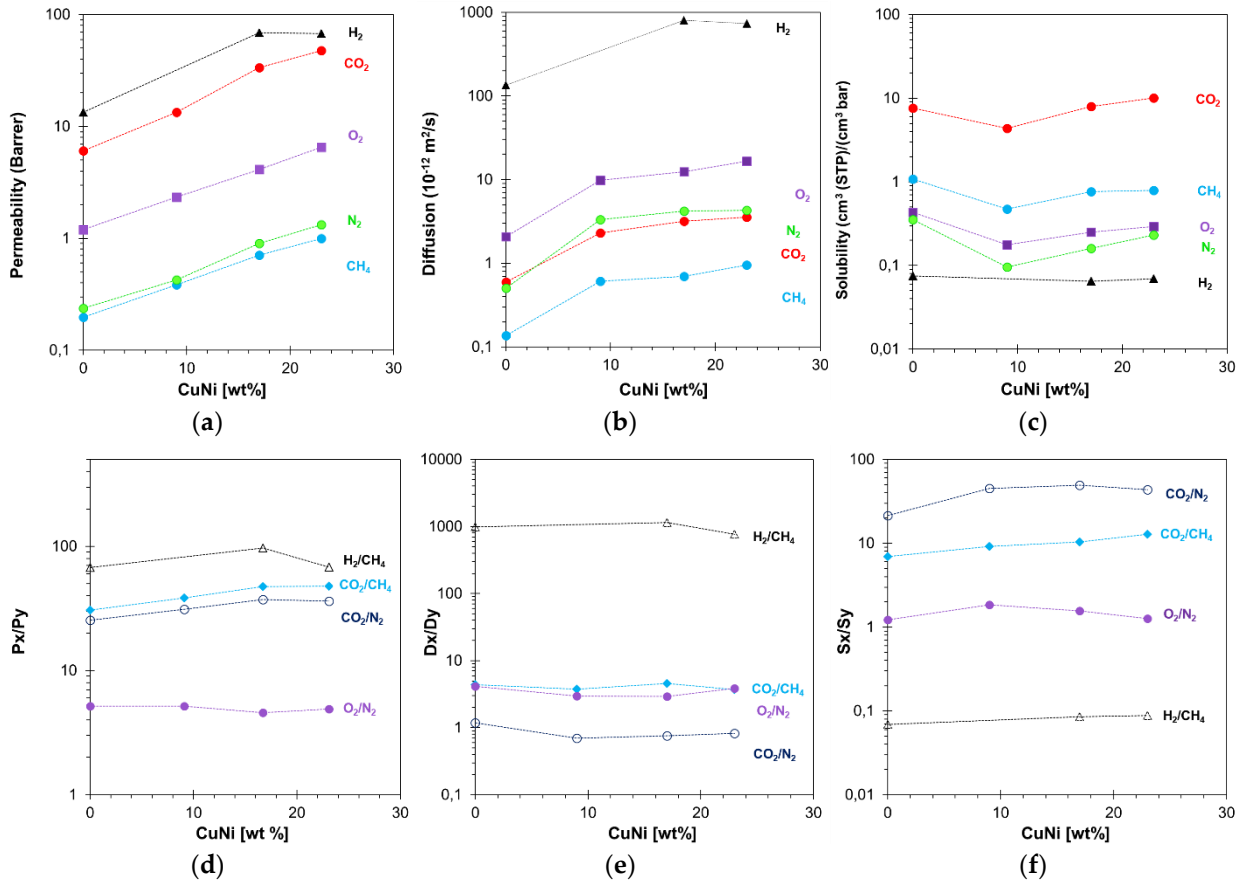

Figure 6. (**a**) Permeability, (**b**) diffusivity, (**c**) solubility coefficients and respective N_2 selectivity (**d, e, f**) for each gas as functions of weight percentage of MOF loaded in PEEK-WC.

For a better understanding of the transport phenomena of gas separation membranes, the diffusion and solubility coefficients are often correlated with the molecular properties of gases [54]. Both neat polymers show a linear dependency of the diffusivity (D) on the squared gas diameter (d^2_{eff}) (Figure 7a and b), suggesting that the gas transport in neat polymers follows the diffusion solution model. In the presence of the MOF, both polymers show non-linearity of the D *vs* d^2_{eff} correlation (Figure 7), which becomes more evident at higher MOF loading. A similar trend was recently observed for PIMs [55], where it was attributed to a different size-selectivity for small and large gas species due to the highly interconnected free volume. These results suggest that the CuNi-MOF particles with their internal void structure have a similar effect on the gas diffusion of Pebax®1657 and PEEK-WC, introducing preferential diffusion pathways into the system, which change the main transport mechanism especially for the small molecules. As described above, the remarkably lower effective diffusion in Pebax®1657 is due to the much higher sorption capacity of the MOFs, than of the neat Pebax®1657 [39]. Only for the CO_2/N_2 gas pair, there is a remarkable inversion from preferential N_2 diffusion in the neat pebax, to preferential CO_2 diffusion for the sample with the highest MOF concentration. Instead, in the glassy PEEK-WC, with much lower intrinsic diffusion coefficients in the neat polymer, the MOF has a strong positive effect on the total permeability of the mixed matrix membrane due to the far more rapid diffusion through the cages of the MOFs. In PEEK-WC, after an initial decrease compared to the neat polymer, the solubility of all gases increases with the CuNi-MOF concentration. This is similar to what was observed in Pebax, but only in PEEK-WC this leads to an increasing permeability, due to the positive effect on the diffusivity as well.

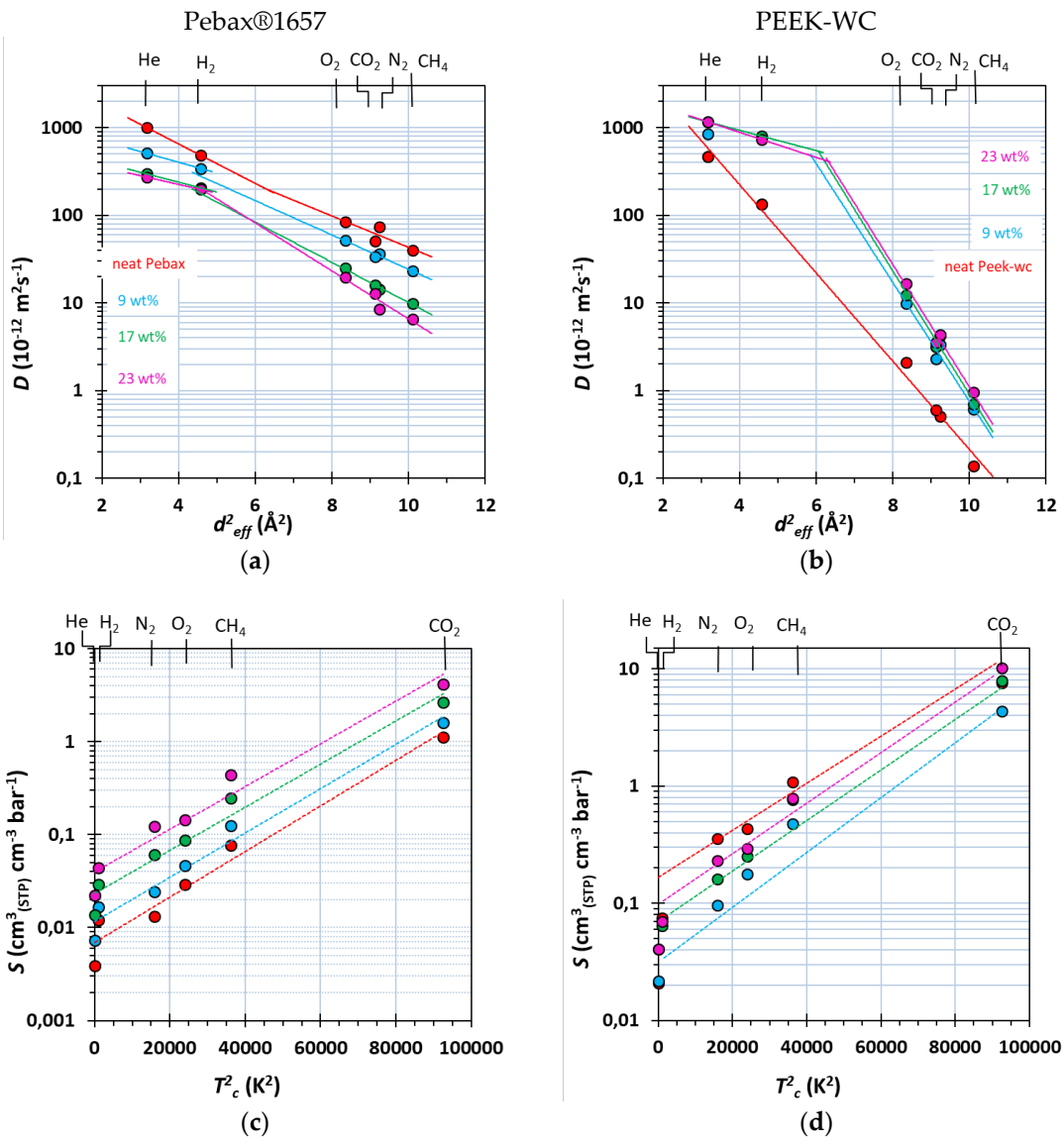

Figure 7. Correlation of the effective diffusion coefficient as a function of the molecular diameter of six light gases in **(a)** Pebax®1657/CuNi MMMs and **(b)** PEEK-WC/CuNi MMMs. Correlation of the effective solubility coefficient of the gases as a function of their critical temperature in **(c)** Pebax®1657/CuNi MMMs and **(d)** PEEK-WC/CuNi MMMs. The legend is identical in all individual graphs.

3.4 Mixed gas transport properties

Mixed gas permeation measurements were carried out on the representative membranes with the highest MOF concentration in each polymer in view of two relevant industrial gas separations, namely biogas upgrading and CO_2 capture from flue gas, involving CO_2 separation from CH_4 and N_2, respectively (Figure 8). For this propose, measurements were performed from 1 to 6 bar(a) with simulated flue gas (CO_2/N_2, 15/85 vol%) and simulated biogas (CO_2/CH_4, 35/65 vol%). The glassy PEEK-WC MMM exhibits typical dual mode behaviour with the CO_2/CH_4 mixture, showing a decrease of CO_2 permeability as a function of the increased feed pressure, which causes a simultaneous and slightly smaller decrease of CO_2/CH_4 selectivity. This indicates that the free volume in the PEEK-WC phase and in the MOFs' pores is gradually becoming occupied by CO_2, and as a result, the CH_4 permeability slightly decreases as a function of pressure. Moreover, some hysteresis of CO_2 and CH_4 permeability is observed when reducing the pressure after the initial pressure increase steps. This is ascribed to a slight CO_2-induced dilation of the polymer, leaving a higher free

volume when the pressure is decreased, and thus a higher CH_4 permeability and a slightly lower selectivity. In the separation of the CO_2/N_2 mixture no further hysteresis takes place because of the lower CO_2 partial pressure, for the same reason the CO_2 permeability is slightly higher than in the biogas mixture.

Contrary to the glassy PEEK-WC, the rubbery Pebax®1657/CuNi-MOF (23 wt%) membrane shows essentially pressure-independent permeability and selectivity (Figure 8a), after only a slight increase in permeability with pressure in the first run, apparently due to a certain conditioning of the sample. The transport properties of the Pebax-based membrane are dominated by the rubbery phase, and the dispersed MOFs only provide a higher gas sorption capacity in the membrane but do not significantly affect the overall performance.

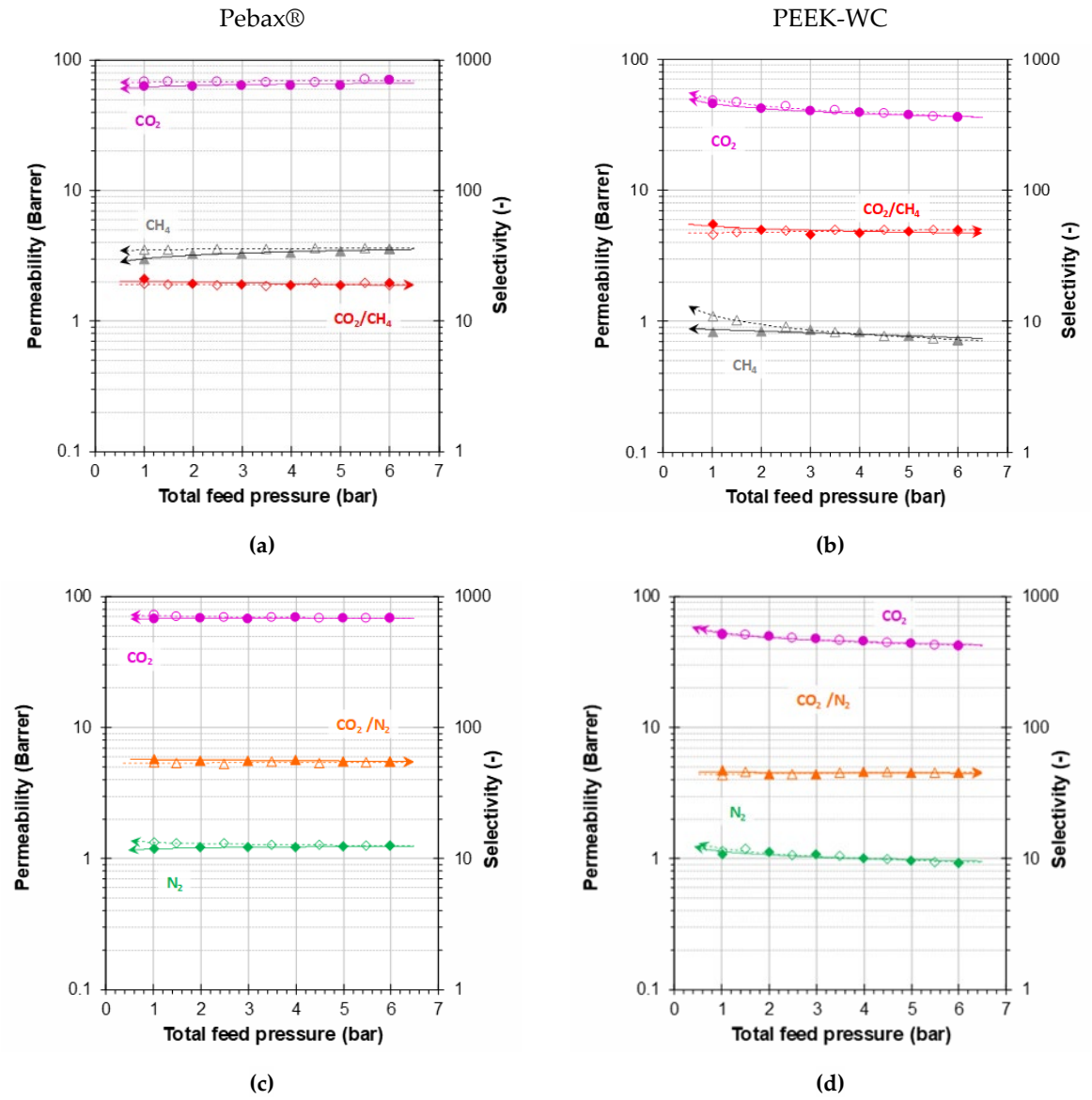

Figure 8. Pressure dependence of CO_2 and CH_4 permeabilities and CO_2/CH_4 selectivity using the binary mixture of CO_2/CH_4 (35:65 vol%) for Pebax®1657_23 wt% CuNi-MOF (**a**) and PEEK-WC_23% CuNi-MOF (**b**). Pressure dependence of CO_2 and N_2 permeabilities and CO_2/N_2 selectivity in binary mixture conditions for CO_2/N_2 (15:85 vol%) of Pebax®1657_23 wt% CuNi (**c**) and PEEK-WC_23% CuNi (**d**). Closed symbols for stepwise increase of the pressure and open symbols for the subsequent stepwise decrease of the pressure. Trend lines are plotted as a guide to the eye.

3.5 Robeson's plots and performance overview

The gas transport properties for all membranes are summarized in the Robeson diagrams in Figure 9 for four gas pairs representing industrially important separations: CO_2/N_2, CO_2/CH_4, O_2/N_2 and H_2/N_2.

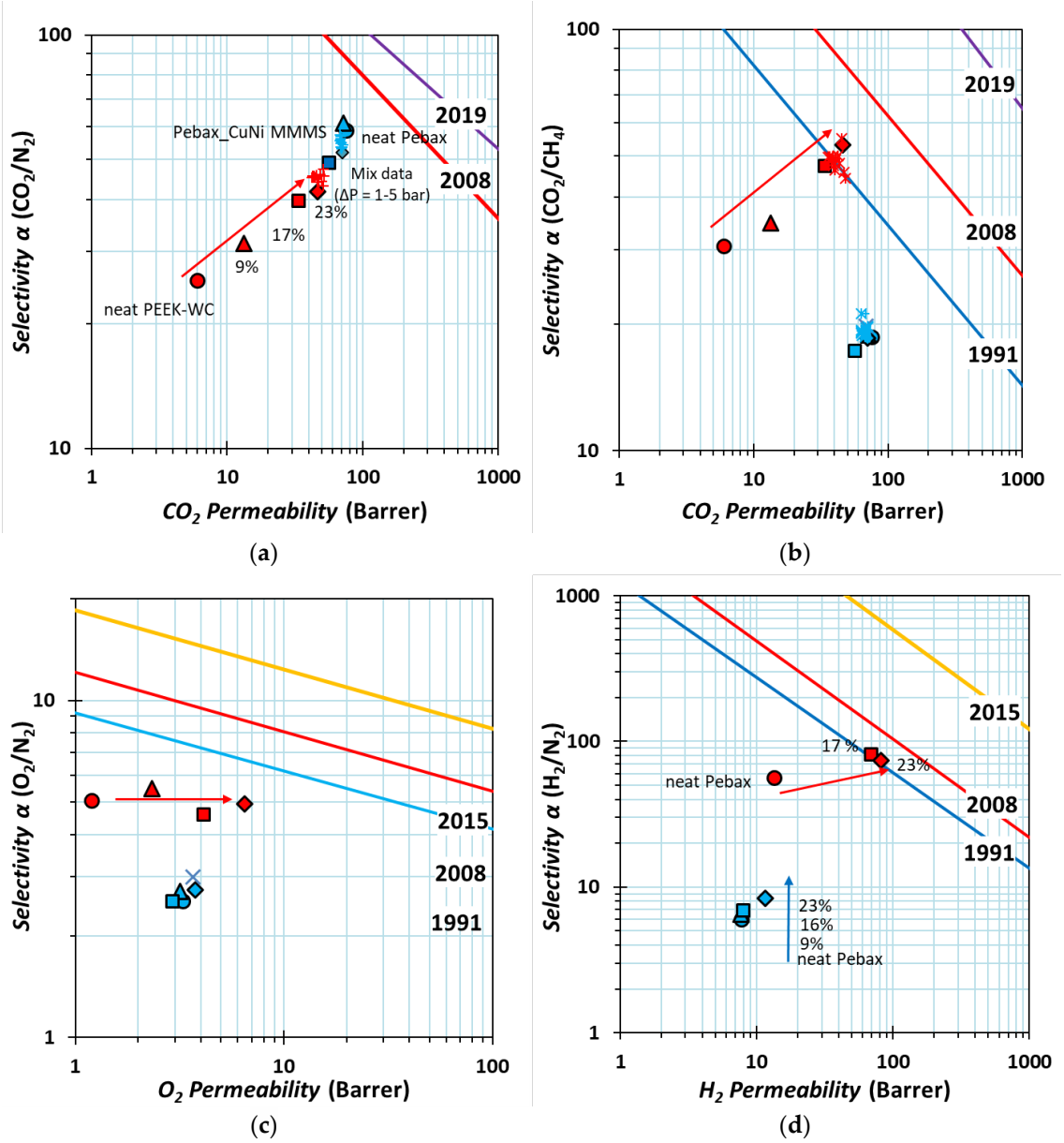

Figure 9. Robeson's plots for CO_2/N_2 (**a**) CO_2/CH_4 (**b**) O_2/N_2 (**c**) H_2/N_2 (**d**) showing the data of Pebax1657/CuNi (blue) and PEEK-WC/CuNi at different MOF loadings of 0 wt% (= neat polymers, ●,●), 9 wt% (▲,▲),17 wt% (■,■) and 23 wt% (♦,♦). Blue line 1991 upper bound, red line 2008 upper bound [8,9]; yellow line 2015 [56]; purple line 2019 upper bound [57]. The arrows qualitatively indicate the direction of increasing MOF loading. The clouds of blue "X" and red "X" symbols represent the mixed gas data in the pressure range of 1-6 bar for Pebax1657/CuNi-MOF at 29 wt% and PEEK-WC/CuNi-MOF at 23 wt% of MOF loading. Please refer to the electronic version for colour figures.

For all gases except H_2, the neat rubbery Pebax®1657 is more permeable than neat glassy PEEK-WC. On the other hand, PEEK-WC is more selective than Pebax®1657 for all gas pairs, except for the CO_2/N_2 separation (Figure 9a). For the CO_2/N_2 gas pair, with nearly identical diameter of the molecules, the selectivity is almost entirely due to solubility selectivity, which is higher in Pebax then in PEEK-WC. However, whereas CuNi-MOF in Pebax®1657 has a marginal effect, CuNi-MOF in the

glassy PEEK-WC, increases drastically not only the CO_2/N_2 selectivity (from 25 to 37), but also the CO_2 permeability (from 6 to ~50 Barrer), near the CO_2 permeability of the rubbery Pebax®1657 (PCO_2 ~69 Barrer) (Figure 9a).

For CO_2/CH_4 separation, the PEEK-WC-based MMMs show far superior properties than the Pebax®-based membranes, which hardly change with the MOF concentration. A strong contribution of size selectivity between CO_2 and the much bulkier CH_4 molecules (Figure 7b) and a further increase of both solubility and diffusivity with increasing MOF concentration leads to enhanced selectivity (from 30 to ~ 50, above that of Pebax) and CO_2 permeability (from 6 to ~50 Barrer), exceeding the 1991 Robeson upper bound. For both mixtures, the performance is very similar to the ideal selectivity and pure gas permeability, indicating the absence of significant coupling effect (Figure 9b).

The O_2/N_2 separation (Figure 9c) is mainly due to diffusion selectivity. Neither the permeability, nor the selectivity changes much in Pebax®1657 upon addition of CuNi-MOF, but in PEEK-WC the permeability of both gases increases 5-fold in the presence of 23 wt% CuNi-MOF, maintaining an almost constant O_2/N_2 selectivity.

Finally, the trend for H_2/N_2 separation is similar to that of O_2/N_2, but in this case for both polymers the MOFs also have a slightly higher H_2/N_2 selectivity than the neat polymers, as a result of increased diffusion selectivity. The H_2 permeability in Pebax® 1657 slightly increases from 8 to 11 Barrer, and the H_2/N_2 selectivity and permeability in the PEEK-WC/CuNi-MOF MMMs both strongly increase, surpassing the 1991 upper bound.

4. Conclusions

Development of novel, well performing gas separation membranes requires good understanding of their transport properties. This is even more important for complex systems such as mixed matrix membranes in which a porous filler is dispersed in the polymer matrix. Therefore, this work describes the comparison of the performance of two sets of membranes, glassy PEEK-WC membranes and rubbery Pebax®1657 membranes, with different concentrations of an oxamate-based CuNi-MOF. An increase of the Young's modulus for both membrane sets confirms that the MOF increases the stiffness of the polymer. In the case of the Pebax®1657 membrane, this is also accompanied by a slight shift of the melting peak of the PEO phase to higher temperatures, which suggests a good interaction of the MOF with the PEO phase. On the other hand, the presence of the MOF reduces the melting enthalpy and thus the overall crystallinity of both the PEO phase and the PA phase of Pebax®, whereas it does not affect the glass transition temperature of PEEK-WC. Only for PEEK-WC, along with Young's modulus also the tensile strength increases, but for both polymers the maximum deformation decreases with the addition of the MOF.

In terms of transport properties, the permeability of PEEK-WC strongly increases with increasing MOF content, mostly due to an increase in the effective diffusion coefficient, whereas unexpectedly, the effective diffusion coefficient in Pebax®1657 drastically decreases upon addition of the MOF. This is almost completely compensated by an increase in solubility, so that the permeability remains nearly constant. The increase in diffusivity favours especially the smaller gas species, and as a result, the PEEK-WC MMMs show a simultaneous increase in CO_2 permeability and CO_2/CH_4 selectivity, and the membranes with the highest MOF loading approach Robeson's 2008 upper bounds for these gas pairs. In the range of 1-6 bar(a), the mixed gas permeation tests with CO_2/N_2 15/85 vol% and CO_2/CH_4 35/65 vol% mixtures show only a weak pressure-dependence for the CO_2/CH_4 mixture in PEEK-WC with 30% MOF, typical for materials with dual mode sorption behavior, but not for the CO_2/N_2 mixture in PEEK-WC and for both mixtures in the Pebax-based MMMs.

Summarizing, the detailed analysis of the gas transport properties of the two series of MMMs highlights the enormous impact of the polymer matrix on the effectiveness of the same MOF when it is embedded in a rubbery or a glassy polymer. Even if the MOF improves significantly the gas solubility, this may not have a positive effect on the permeability if the diffusivity is not increased simultaneously. Successful development of better-performing MMMs can therefore not rely on studies of only the overall permeability, but necessitates knowledge of the individual solubility and

diffusion coefficient. For both parameters, the values of the polymer and the porous filler should be carefully matched to yield optimum performance.

Acknowledgments: Phenom-World B.V., Eindhoven (NL), is gratefully acknowledged for providing a Phenom Pro X desktop SEM for evaluation. R.B. thanks the MIUR (project PON R&I FSE-FESR 2014-2020) for predoctoral grants.

Supplementary Materials: The following are available online at: , **Table SI-1**. List of MMMs prepared. Fig. S-1 EDX of Pebax®1657/CuNi-MOF (a) and PEEK-WC/CuNi-MOF (b) at an accelerating voltage of 15Kv. **Fig. S-2** SEM images of cross section for MMMs of Pebax®1657/CuNi-MOF and PEEK-WC/CuNi-MOF. **Table S-2** Pure gas permeability, solubility and diffusion coefficients, and respective selectivity for neat Pebax1657 and Pebax1657/CuNi MMMs. **Table S-3** Pure gas permeability, solubility and diffusion coefficients, and respective selectivity for neat PEEK-WC and PEEK-WC/CuNi MMMs. **Table S-4** Mixed gas permeabilities and selectivities of PEEK-WC/CuNi 23 wt% membrane using binary mixture CO2/CH4 (35/65) at pressure of 1-6 bar. **Table S-5** Mixed gas permeabilities and selectivities of PEEK-WC/CuNi 23 wt% membrane using binary mixture CO2/N2 (15/85) at pressure of 1-6 bar.

Author Contributions: E.E. and R. B. conceived, designed and performed the membrane preparation and characterization experiments under the supervision of J.C.J and D.A.; J.F. S and E.P synthetized and provided CuNi-MOF; E.E. and A. F. performed the single gas permeation and DSC experiments; E. E. and J.C.J. performed mechanical tests. M.M. performed the mixed gas permeation experiments under the supervision of J.C.J. All authors analyzed the data and wrote the paper with similar effort.

Funding: This work was supported by Ministero dell'Istruzione, dell'Università e della Ricerca (Italy). Phenom-World B.V., Eindhoven (NL), is gratefully acknowledged for providing a Phenom Pro X desktop SEM for evaluation. Dr. C. Cantoni (Arkema Italy) is gratefully acknowledged for providing the Pebax®1657 pellets.

Conflicts of Interest: The authors declare no conflict of interest.

References

1. Ockwig, N.W.; Nenoff, T.M. Membranes for hydrogen separation. *Chem. Rev.* 2007.
2. Himma, N.F.; Wardani, A.K.; Prasetya, N.; Aryanti, P.T.P.; Wenten, I.G. Recent progress and challenges in membrane-based O2/N2 separation. *Rev. Chem. Eng.* **2019**.
3. Coombe, H.S.; Nieh, S. Polymer membrane air separation performance for portable oxygen enriched combustion applications. *Energy Convers. Manag.* **2007**.
4. Chen, X.Y.; Vinh-Thang, H.; Ramirez, A.A.; Rodrigue, D.; Kaliaguine, S. Membrane gas separation technologies for biogas upgrading. *RSC Adv.* 2015.
5. Esposito, E.; Dellamuzia, L.; Moretti, U.; Fuoco, A.; Giorno, L.; Jansen, J.C. Simultaneous production of biomethane and food grade CO 2 from biogas: an industrial case study. *Energy Environ. Sci.* **2019**, *12*, 281–289.
6. Galizia, M.; Chi, W.S.; Smith, Z.P.; Merkel, T.C.; Baker, R.W.; Freeman, B.D. 50th Anniversary Perspective: Polymers and Mixed Matrix Membranes for Gas and Vapor Separation: A Review and Prospective Opportunities. *Macromolecules* **2017**, *50*, 7809–7843.
7. Brunetti, A.; Scura, F.; Barbieri, G.; Drioli, E. Membrane technologies for CO2 separation. *J. Memb. Sci.* **2010**.
8. Robeson, L.M. The upper bound revisited. *J. Memb. Sci.* **2008**, *320*, 390–400.
9. Robeson, L.M. Correlation of separation factor versus permeability for polymeric membranes. *J. Memb. Sci.* **1991**, *62*, 165–185.
10. Chuah, C.Y.; Goh, K.; Yang, Y.; Gong, H.; Li, W.; Karahan, H.E.; Guiver, M.D.; Wang, R.; Bae, T.-H.

Harnessing Filler Materials for Enhancing Biogas Separation Membranes. *Chem. Rev.* **2018**, *118*, 8655–8769.

11. Zhu, H.; Liu, D. The synthetic strategies of metal–organic framework membranes, films and 2D MOFs and their applications in devices. *J. Mater. Chem. A* **2019**.
12. Najari, S.; Saeidi, S.; Gallucci, F.; Drioli, E. Mixed matrix membranes for hydrocarbons separation and recovery: a critical review. *Rev. Chem. Eng.* **2019**, *0*.
13. Prasetya, N.; Himma, N.F.; Doddy Sutrisna, P.; Wenten, I.; Ladewig, B.P. A Review on Emerging Organic-containing Microporous Material Membranes for Carbon Capture and Separation. *Chem. Eng. J.* **2019**, 123575.
14. Ebadi Amooghin, A.; Mashhadikhan, S.; Sanaeepur, H.; Moghadassi, A.; Matsuura, T.; Ramakrishna, S. Substantial breakthroughs on function-led design of advanced materials used in mixed matrix membranes (MMMs): A new horizon for efficient CO2 separation. *Prog. Mater. Sci.* **2019**, *102*, 222–295.
15. Review, A. Performance of Mixed Matrix Membranes Containing Three-Dimensional (3D) Fillers for CO 2 Separation : **2018**.
16. Cohen, S.M. The Postsynthetic Renaissance in Porous Solids. *J. Am. Chem. Soc.* **2017**, *139*, 2855–2863.
17. Fortea-Pérez, F.R.; Mon, M.; Ferrando-Soria, J.; Boronat, M.; Leyva-Pérez, A.; Corma, A.; Herrera, J.M.; Osadchii, D.; Gascon, J.; Armentano, D.; et al. The MOF-driven synthesis of supported palladium clusters with catalytic activity for carbene-mediated chemistry. *Nat. Mater.* **2017**, *16*, 760–766.
18. Mon, M.; Tiburcio, E.; Ferrando-Soria, J.; Gil San Millán, R.; Navarro, J.A.R.; Armentano, D.; Pardo, E. A post-synthetic approach triggers selective and reversible sulphur dioxide adsorption on a metal-organic framework. *Chem. Commun.* **2018**, *54*, 9063–9066.
19. Jansen, J.C.; Drioli, E. Poly(ether ether ketone) derivative membranes—a review of their preparation, properties and potential. *Polym. Sci. Ser. A* **2009**, *51*, 1355–1366.
20. Tasselli, F.; Jansen, J.C.; Drioli, E. PEEKWC Ultrafiltration Hollow-Fiber Membranes: Preparation, Morphology, and Transport Properties. *J. Appl. Polym. Sci.* **2004**, *91*, 841–853.
21. Buonomenna, M.G.; Figoli, A.; Jansen, J.C.; Drioli, E. Preparation of Asymmetric PEEKWC Flat Membranes with Different Microstructures by Wet Phase Inversion. *J. Appl. Polym. Sci.* **2004**, *92*, 576–591.
22. Jansen, J.C.; Buonomenna, M.G.; Figoli, A.; Drioli, E. Asymmetric membranes of modified poly(ether ether ketone) with an ultra-thin skin for gas and vapour separations. *J. Memb. Sci.* **2006**, *272*, 188–197.
23. Iulianelli, A.; Algieri, C.; Donato, L.; Garofalo, A.; Galiano, F.; Bagnato, G.; Basile, A.; Figoli, A. New PEEK-WC and PLA membranes for H2 separation. *Int. J. Hydrogen Energy* **2017**, *42*, 22138–22148.
24. Iulianelli, A.; Clarizia, G.; Gugliuzza, A.; Ebrasu, D.; Bevilacqua, A.; Trotta, F.; Basile, A. Sulfonation of PEEK-WC polymer via chloro-sulfonic acid for potential PEM fuel cell applications. *Int. J. Hydrogen Energy* **2010**, *35*, 12688–12695.
25. Clarizia, G.; Algieri, C.; Regina, A.; Drioli, E. Zeolite-based composite PEEK-WC membranes: Gas transport and surface properties. *Microporous Mesoporous Mater.* **2008**, *115*, 67–74.
26. Xin, Q.; Liu, T.; Li, Z.; Wang, S.; Li, Y.; Li, Z.; Ouyang, J.; Jiang, Z.; Wu, H. Mixed matrix membranes composed of sulfonated poly(ether ether ketone) and a sulfonated metal–organic framework for gas separation. *J. Memb. Sci.* **2015**, *488*, 67–78.
27. Esposito, E.; Clarizia, G.; Bernardo, P.; Jansen, J.C.; Sedláková, Z.; Izák, P.; Curcio, S.; Cindio, B. de; Tasselli, F. Pebax®/PAN hollow fiber membranes for CO2/CH4 separation. *Chem. Eng. Process. Process Intensif.* **2015**, *94*, 53–61.

28. Kim, K.; Ingole, P.G.; Kim, J.; Lee, H. Separation performance of PEBAX/PEI hollow fiber composite membrane for SO2/CO2/N2 mixed gas. *Chem. Eng. J.* **2013**, *233*, 242–250.
29. Asghari, M.; Mosadegh, M.; Riasat Harami, H. Supported PEBA-zeolite 13X nano-composite membranes for gas separation: Preparation, characterization and molecular dynamics simulation. *Chem. Eng. Sci.* **2018**, *187*, 67–78.
30. Dai, Z.; Bai, L.; Hval, K.N.; Zhang, X.; Zhang, S.; Deng, L. Pebax®/TSIL blend thin film composite membranes for CO2 separation. *Sci. China Chem.* **2016**, *59*, 1–9.
31. Ehsani, A.; Pakizeh, M. Synthesis, characterization and gas permeation study of ZIF-11/Pebax® 2533 mixed matrix membranes. *J. Taiwan Inst. Chem. Eng.* **2016**.
32. Jomekian, A.; Bazooyar, B.; Behbahani, R.M.; Mohammadi, T.; Kargari, A. Ionic liquid-modified Pebax® 1657 membrane filled by ZIF-8 particles for separation of CO2 from CH4, N2 and H2. *J. Memb. Sci.* **2017**, *524*, 652–662.
33. Liu, G.; Chernikova, V.; Liu, Y.; Zhang, K.; Belmabkhout, Y.; Shekhah, O.; Zhang, C.; Yi, S.; Eddaoudi, M.; Koros, W.J. Mixed matrix formulations with MOF molecular sieving for key energy-intensive separations. *Nat. Mater.* **2018**, *17*, 283–289.
34. Jomekian, A.; Behbahani, R.M.; Mohammadi, T.; Kargari, A. High speed spin coating in fabrication of Pebax 1657 based mixed matrix membrane filled with ultra-porous ZIF-8 particles for CO2/CH4 separation. *Korean J. Chem. Eng.* **2016**, *34*, 1–14.
35. Jomekian, A.; Behbahani, R.M.; Mohammadi, T.; Kargari, A. CO2/CH4 separation by high performance co-casted ZIF-8/Pebax 1657/PES mixed matrix membrane. *J. Nat. Gas Sci. Eng.* **2016**, *31*, 562–574.
36. Atash Jameh, A.; Mohammadi, T.; Bakhtiari, O. Preparation of PEBAX-1074/modified ZIF-8 nanoparticles mixed matrix membranes for CO2 removal from natural gas. *Sep. Purif. Technol.* **2020**, *231*, 115900.
37. Meshkat, S.; Kaliaguine, S.; Rodrigue, D. Mixed matrix membranes based on amine and non-amine MIL-53(Al) in Pebax® MH-1657 for CO2 separation. *Sep. Purif. Technol.* **2018**, *200*, 177–190.
38. Noroozi, Z.; Bakhtiari, O. Preparation of Amino Functionalized Titanium Oxide Nanotubes and Their Incorporation within Pebax/PEG Blended Matrix for CO2/CH4 Separation. *Chem. Eng. Res. Des.* **2019**.
39. Mon, M.; Bruno, R.; Tiburcio, E.; Grau-Atienza, A.; Sepúlveda-Escribano, A.; V Ramos-Fernandez, E.; Fuoco, A.; Esposito, E.; Monteleone, M.; Carolus Jansen, J.; et al. Efficient Gas Separation and Transport Mechanism in Rare Hemilabile Metal-Organic Framework. *Chem. Mater.* **2019**, *0*, null-null.
40. Song, C.; Li, R.; Fan, Z.; Liu, Q.; Zhang, B.; Kitamura, Y. CO2/N2 separation performance of Pebax/MIL-101 and Pebax /NH2-MIL-101 mixed matrix membranes and intensification via sub-ambient operation. *Sep. Purif. Technol.* **2020**, *238*, 116500.
41. Sutrisna, P.D.; Hou, J.; Zulkifli, M.Y.; Li, H.; Zhang, Y.; Liang, W.; D'Alessandro, D.M.; Chen, V. Surface functionalized UiO-66/Pebax-based ultrathin composite hollow fiber gas separation membranes. *J. Mater. Chem. A* **2018**, *6*, 918–931.
42. Kim, J.; Choi, J.; Soo Kang, Y.; Won, J. Matrix effect of mixed-matrix membrane containing CO<inf>2</inf>-selective MOFs. *J. Appl. Polym. Sci.* **2016**, *133*, 1–8.
43. Grancha, T.; Ferrando-Soria, J.; Zhou, H.C.; Gascon, J.; Seoane, B.; Pasán, J.; Fabelo, O.; Julve, M.; Pardo, E. Postsynthetic Improvement of the Physical Properties in a Metal-Organic Framework through a Single Crystal to Single Crystal Transmetallation. *Angew. Chemie - Int. Ed.* **2015**, *54*, 6521–6525.
44. Jansen, J.C.; Friess, K.; Drioli, E. Organic vapour transport in glassy perfluoropolymer membranes: A simple semi-quantitative approach to analyze clustering phenomena by time lag measurements. *J.*

Memb. Sci. **2011**, *367*, 141–151.

45. Crank, J. *The mathematics of diffusion*; 2nd ed.; Clarendon Press: Oxford, 1975; ISBN 0198533446.
46. Fraga, S.C.; Monteleone, M.; Lanč, M.; Esposito, E.; Fuoco, A.; Giorno, L.; Pilnáček, K.; Friess, K.; Carta, M.; McKeown, N.B.; et al. A novel time lag method for the analysis of mixed gas diffusion in polymeric membranes by on-line mass spectrometry: Method development and validation. *J. Memb. Sci.* **2018**, *561*, 39–58.
47. Fernandes, T.S.; Melo, W.D.C.; Kalinke, L.H.G.; Rabelo, R.; Valdo, A.K.; Da Silva, C.C.; Martins, F.T.; Amorós, P.; Lloret, F.; Julve, M.; et al. 2D and 3D mixed MII/CuII metal-organic frameworks (M = Ca and Sr) with: N, N ′-2,6-pyridinebis(oxamate) and oxalate: Preparation and magneto-structural study. *Dalt. Trans.* **2018**, *47*, 11539–11553.
48. Khosravi, T.; Omidkhah, M.; Kaliaguine, S.; Rodrigue, D. Amine-functionalized CuBTC/poly(ether-b-amide-6) (Pebax® MH 1657) mixed matrix membranes for CO2/CH4 separation. *Can. J. Chem. Eng.* **2017**, *95*, 2024–2033.
49. Luo, H.; Vaivars, G.; Mathe, M. Cross-linked PEEK-WC proton exchange membrane for fuel cell. *Int. J. Hydrogen Energy* **2009**, *34*, 8616–8621.
50. Li, W.; Galiano, F.; Estager, J.; Monbaliu, J.C.M.; Debecker, D.P.; Figoli, A.; Luis, P. Sorption and pervaporation study of methanol/dimethyl carbonate mixture with poly(etheretherketone) (PEEK-WC) membrane. *J. Memb. Sci.* **2018**, *567*, 303–310.
51. Longo, M.; De Santo, M.P.; Esposito, E.; Fuoco, A.; Monteleone, M.; Giorno, L.; Jansen, J.C. Force spectroscopy determination of Young's modulus in mixed matrix membranes. *Polymer (Guildf).* **2018**, *156*, 22–29.
52. Paul, D.R. Effect of immobilizing adsorption on the diffusion time lag. *J. Polym. Sci. Part A-2 Polym. Phys.* **1969**, *7*, 1811–1818.
53. Grzywna, Z.; Podkowka, J. Effect of immobilizing adsorption on mass transport through polymer films. *J. Memb. Sci.* **1981**, *8*, 23–31.
54. Yampolskii, Y. Polymeric Gas Separation Membranes. **2012**, *45*, 3298–3311.
55. Fuoco, A.; Rizzuto, C.; Tocci, E.; Monteleone, M.; Esposito, E.; Budd, P.M.; Carta, M.; Comesaña-Gándara, B.; McKeown, N.B.; Jansen, J.C. The origin of size-selective gas transport through polymers of intrinsic microporosity. *J. Mater. Chem. A* **2019**, *7*, 20121–20126.
56. Swaidan, R.; Ghanem, B.; Pinnau, I. Fine-Tuned Intrinsically Ultramicroporous Polymers Redefine the Permeability/Selectivity Upper Bounds of Membrane-Based Air and Hydrogen Separations. *ACS Macro Lett.* **2015**, *4*, 947–951.
57. Comesana-Gandara, B.; Chen, J.; Bezzu, C.G.; Carta, M.; Rose, I.; Ferrari, M.-C.; Esposito, E.; Fuoco, A.; McKeown, N.B.; Jansen, J.C. Redefining the Robeson upper bounds for CO2/CH4 and CO2/N2 separations using a series of ultrapermeable benzotriptycene-based Polymers of Intrinsic Microporosity. *Submitt. to Energy Environ. Sci.* **2019**.